Tomasz RYMARCZYK[1,2], Jan SIKORA[2]

Research & Development Centre Netrix S.A. (1), University of Economics and Innovation in Lublin (2)

doi:10.15199/48.2020.02.21

Optimization Method and PCA noise suppression application for Ultrasound Transmission Tomography

Abstract. *In this paper, the new version of imaging algorithm for Ultrasound Transmission Tomography was presented. This algorithm was comprehensively tested with both synthetic and real measurement data. Different configuration of an internal objects were considered. In order to improve the quality of imaging the input data were treated by Principal Component Analysis. The algorithm proved its usefulness and its weak sides which have to be improved in the future.*

Streszczenie. *W tym artykule przedstawiono nową wersję algorytmu w Ultradźwiękowej Tomografii Transmisyjnej. Przedstawiony algorytm był wszechstronnie przetestowany zarówno dla danych syntetycznych jak i na danych pomiarowych dla różnych konfiguracji obiektów wewnętrznych. W celu poprawienia jakości obrazowania, dane wejściowe poddane zostały Analizie Składowych Głównych. Zaproponowany algorytm wykazał się swoją użytecznością a także ujawnił swoje słabe strony, które w przyszłości mogą zostać usunięte.(**Metoda optymalizacji i redukcja szumu PCA do ultradźwiękowej tomografii transmisyjnej**)*

Słowa kluczowe: Transmisyjna Tomografia Ultradźwiękowa, Obrazowanie, Optymalizacja, Liniowe Ograniczenia Nierównościowe, Analiza Składowych Głównych.
Keywords: Ultrasound Transmission Tomography, Image Reconstruction, Optimization, Linear Inequality Constrains, Principal Component Analysis.

Introduction

The idea of optimization approach [1-11], among the others [12-16] is very popular for the inverse problem's solution [17-19] and could be successfully applied in ultrasonic image reconstruction [20,21]. The paper concentrates on reconstruction algorithm based on synthetic and on real measurements provided by Netrix R&D company.

The NETRIX tomograph [22] is working in transmission mode [23,24], so reflection signals are not measured. In this work all, simplifying assumption was introduced along with the fact that ultrasound wave is propagated along the strait lines.

The problem solution is started with a certain number of the trial objects, randomly or rather with the certain algorithm, distributed inside the investigated region. Such a location of the candidate objects we will call the generalized starting point to the optimization process.

The generalized starting point idea consists on the assumption that the object which is sought could be everywhere inside the region.

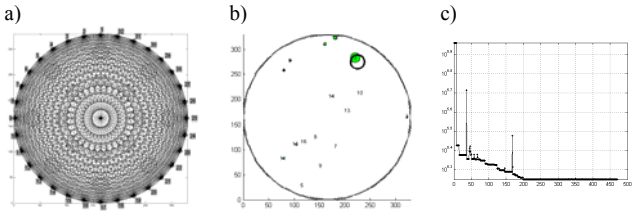

Fig. 1: Generalized starting point. a) Candidates internal objects with the ray's distribution. b) Results of the imaging and the real position of internal object denoted by black circle. c) The optimization processes

So, in such case, knowing that the cross section of the internal object should be a circle, sixteen candidate circular objects are distributed inside the region under consideration as it is shown in Fig. 1a.

The objective function and linear inequality constrain definition

In order to fit calculated signal to the measured signal in each iteration step, the following objective function has been defined:

$$(1) \qquad \Phi=\sum_{j=1}^{j=p}\Phi_j=\frac{1}{2}\sum_{j=1}^{j=p}\left(\mathbf{f}_j-\mathbf{v}_{0j}\right)^T\left(\mathbf{f}_j-\mathbf{v}_{0j}\right)=\frac{1}{2}\left(\mathbf{F}-\mathbf{V}_0\right)^T\left(\mathbf{F}-\mathbf{V}_0\right)$$

where: Φ - the total value of objective function calculated for all p=32 or 21 projection angles (positions of the sound sources), $j=1,2,...,p$, Φ_j - objective function for j-th position of the sound source, $\mathbf{f}_j$ - vector (one column matrix) of a sound wave transition times calculated in certain iteration step for assumed distribution of internal objects for the j-th projection angle, $\mathbf{v}_{0j}$ - measured vector of times in μs for the j-th projection angle, and $\mathbf{F}=\left[\mathbf{f}_1,\mathbf{f}_2,...,\mathbf{f}_p\right]^T$, and $\mathbf{V}_0=\left[\mathbf{v}_{01},\mathbf{v}_{02},...,\mathbf{v}_{0p}\right]^T$.

The objective function Φ_j, will be minimized considering given linear inequality constraints [25]. The Φ_j is Mean Squared Error (MSE) of image forming for j-th projection angle. The value of the total objective function for the given measuring data depends on matrix $\mathbf{F}$. The matrix $\mathbf{F}$ is defined in each iteration step by the solution of the forward problem.

Each candidate internal objects possess three parameters defining their position and dimension. So, the total number of decision parameters (optimization parameters) is equal to 16*3=48. For those 48 decision parameters inequality constrains, must be imposed.

Let us assume that the radius of the cross section of the object, must be a positive number along with the length of its position vector. That already complete 32 inequality constrains. Additionally, it could be assumed, however it is not necessary, that the angle of the position vector is positive as well. That increase the number of inequality constraints up to 48.

The inequality constrains protecting against objects overlapping will take the following form:

$$(2) \qquad R_i-r_i-\left(R_{i+1}+r_{i+1}\right)>R_w*0.01$$

where: R_i is the length of the position vector for *i*-th internal object, r_i is the cross section radius of the internal objects (see Fig. 1b).

Finally, the inequality constrains matrix will possess 64 rows and 48 columns.

The internal multi object imaging by optimization approach

The first two sections prove that optimization approach could be useful even in case of the real measurements. The generalized starting point to optimization process proved its flexibility providing nice results (see Fig. 1b). However, those results were achieved for a single obstacle inside the region. So, arise a question if equally good results could be possible to achieve for multi object of internal obstacle.

Let us start with four circular objects the same dimensions as in case considered in the first paragraph. Based on numerical experiment, this time the starting point was consisted with only 8 candidate objects which are shown in yellow colour in Fig. 3a.

As one can observe, during the optimization process, some of the candidate objects were shrank almost to zero (having no influence on final signal - see Fig. 2b) but four of them ideally to slot in the real position of the considered model shown in Fig. 2a.

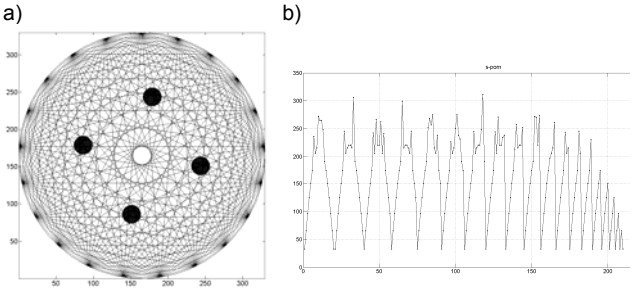

Fig. 2. a) Four internal obstacles. b) Synthetic „measured" noise free signal for 4 internal objects

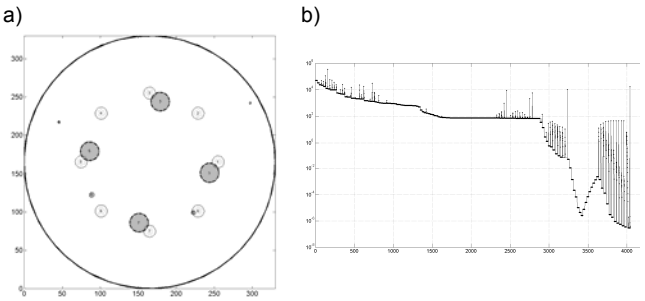

Fig. 3. a) Starting point marked by yellow colour and the final objects in green fitted in the real position of the model marked by dashed blue lines. b) Objective function value versus number of iterations

Referring to the Fig. 1 there are some essential differences. First, the signal is not measured but numerically generated and noise free. Secondly on the perimetry of the region instead 32 sensors we have only 21, causing imagining more difficult. Thanks to the synthetic noise free signal the results are very precise (see Fig. 3a). However, the optimization for that case demanded about 4000 iterations when for the single object and with real measurements only about 450 iteration steps.

To see more clearly the difficulties of multi object imaging by optimization approach regarding the single object, let us consider the proximity effect based on four objects located in the middle of the region (see Fig. 4a). Additionally, the sensitivity has the lowest value in the centre of the region what rise the imaging difficulties. The starting point was the same and the result after about 5000 iteration steps is presented in Fig. 5a.

Always for the tomography problems, a spatial resolution is very important. This algorithm has been tested for that purpose. The multi objects as small as 8 mm in diameter are "visible" for this algorithm. It is less than 2.5% of the diameter of the region under consideration.

The result marked by the green colour is presented in Fig. 5a. One can see the set of objects of the circular shape which are very close to the real position denoted by the blue dashed lines.

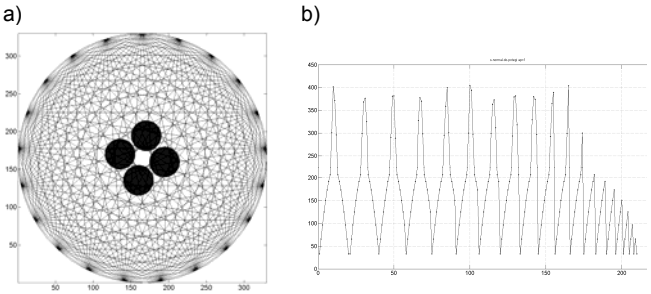

Fig. 4. a) Model for proximity effect. b) Signal „measured" for the proximity case

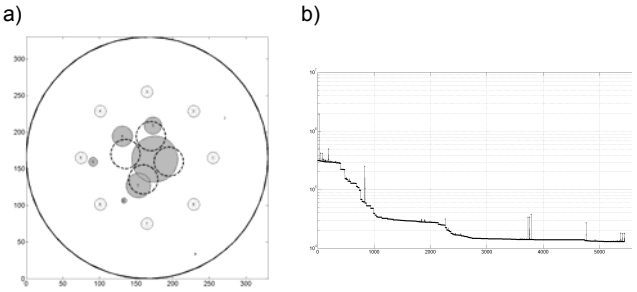

Fig. 5. a) Result of imaging. b) Iterations history

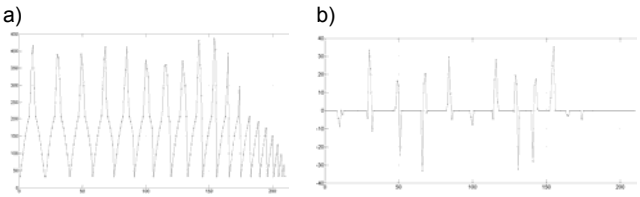

Fig. 6. a) "Measured" signal after iteration process. b) Difference between "measured" signal (Fig. 4b) and the final one (Fig.6a)

This final set is producing the signal presented in Fig. 6a. Discrepancy between "measured" and final signal are shown in Fig. 6b. The maximum discrepancy is 8.75%.

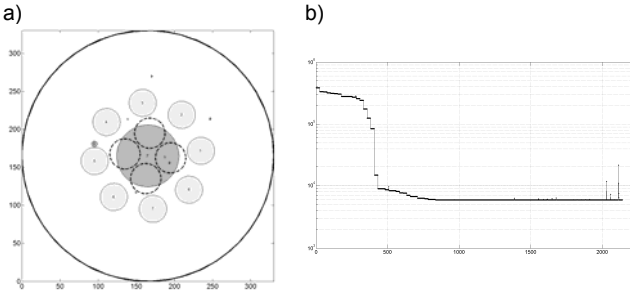

Fig. 7. a) Result of imaging for different starting point. b) Iterations history for a new starting point

It is a common knowledge that the optimization problems are very sensitive on the starting point selection. If the candidate objects become bigger and closer to the

position of the real ones, the solution is different. Now the final image consists of one big obstacle presented in Fig. 7a.

Which solution better fit to the model to be imaged? It is hard to decide as both solutions provide almost the same signal as "measured" one with precision less than 10%.

The internal multi object imaging: the real measurement case

In previous sections algorithm was presented for single object imaging using the real measurements and for more difficult problem like the ones presented in Fig. 2a. For synthetic and noise free data behaviour of the algorithm in case of multi objects was satisfactory. Now it is time to make the next step and move to the imaging with real data for four objects. The region and the location of the objects inside are shown in Fig. 8a [1].

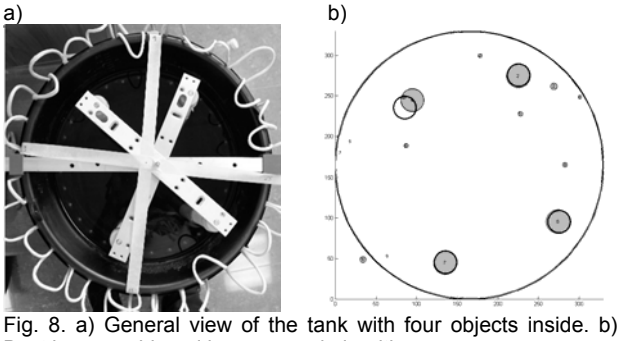

Fig. 8. a) General view of the tank with four objects inside. b) Best image achieved by proposed algorithm

In the Fig. 8b there is the best image which was achieved by proposed algorithm. However, results are not stable. A small change in the starting point or in the inequality constraints cause a dramatic change in the final image. This situation is illustrated in the Fig. 9a.

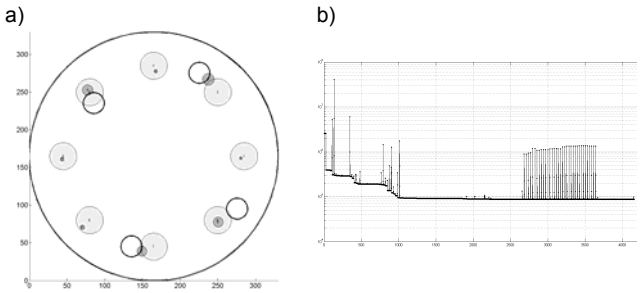

Fig. 9. a) Final image after changing inequality constraints. b) History of optimization

Noise Suppression by The Principal Component Analysis

The Principal Component Analysis (PCA) has three basic applications [26]: 1. pre-processing for empirical modelling, 2. data compression and 3. noise suppression. In this section the third application for the noise suppression will be presented.

The Statistics Toolbox have, the functions like princomp and zscore, but only base MATLAB functions would be used in this paper. The basic idea is that the variance captured by the least important principal components represents noise which should be rejected.

Dropping the last principal components means elimination some of the noise what could improve the ultrasound imaging what is presented in Fig. 10.

This process is like the PCA data compression process with two exception [26]: 1. discarded components have their coefficients set to zero instead of being deleted and 2. the PCA coefficient matrix and its inverse are multiplied together to reduces noise in the data.

As one can see in Fig. 10a are the results without the PCA but Fig. 10b presents results with PCA. Application of PCA produce much better results in comparison to the results without of PCA. However after application of the PCA still one object is missing but the objects sizes are on the edge of "visibility" by the proposed algorithm. The radiuses of the objects are less than 5.6% and still results are not bad.

Looking at the history of the optimization process for the case when PCA is applied the number of iteration is more than two times bigger but the value of the objection function drops one order lower as one can see in the Fig 10b.

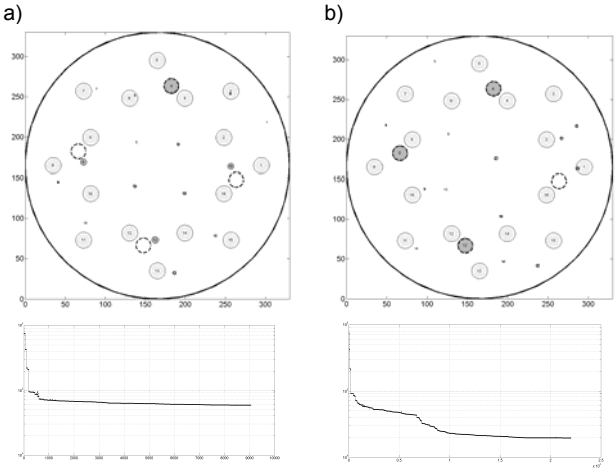

Fig. 10. Results of imaging a) without PCA and b) with PCA

Conclusion

In this paper new algorithm for Ultrasound Transmission Tomography was presented. Based on experiments with numerical and measurements data conclusion can be stated as follows:

1. The algorithm for one internal object provides stable and precise images.
2. For multiple internal objects algorithm has some difficulties to provide stable results.
3. In order to improve the results advanced conditioning of measurements like PCA was applied giving better results.

As a final thoughts, one can say that the PCA is a powerful tool, and is quickly computed on current computers, even on large data. While there are limits to what it can do, it is a handy tool which is inexpensive in terms of compute time.

***Authors**: dr inż. Tomasz Rymarczyk[1,2], e-mail: tomasz@rymarczyk.com, prof. dr hab. inż. Jan Sikora[1,2], e-mail: sik59@wp.pl, 1) Research & Development Centre Netrix S.A., Związkowa 26, 20-148 Lublin, 2) University of Economics and Innovation in Lublin, ul. Projektowa 4, 20-209 Lublin,;*

REFERENCES

[1] Rymarczyk T., "Tomographic Imaging in Environmental, Industrial and Medical Applications", Innovatio Press Publishing Hause, (2019)

[2] Rymarczyk T., Sikora J., Waleska B., Coupled Boundary Element Method and Level Set Function for Solving Inverse Problem in EIT, 7th World Congress on Industrial Process Tomography, WCIPT7, (2013), 312-319

[3] Smolik W., Forward Problem Solver for Image Reconstruction by Nonlinear Optimization in Electrical Capacitance Tomography, Flow Measurement and Instrumentation, (2010), vol. 21, 70–77

[4] Soleimani M., Mitchell C.N., Banasiak R., Wajman R., Adler A., Four-dimensional electrical capacitance tomography imaging using experimental data, Progress in Electromagnetics Research, (2009), vol. 90, 171-186
[5] Rymarczyk, T.; Kozłowski, E.; Kłosowski, G.; Niderla, K. Logistic Regression for Machine Learning in Process Tomography. Sensors, 19 (2019), 3400.
[6] Romanowski, A.; Łuczak, P.; Grudzień, K. X-ray Imaging Analysis of Silo Flow Parameters Based on Trace Particles Using Targeted Crowdsourcing. Sensors, 19 (2019), No. 15, 3317;
[7] Kozlowski, Edward; Mazurkiewicz, Dariusz; Kowalska, Beata; et al., Binary Linear Programming as a Decision-Making Aid for Water Intake Operators, 1st International Conference on Intelligent Systems in Production Engineering and Maintenance, Wroclaw, Poland 28-29.09.2017, Intelligent systems in production engineering and maintenance (ISPEM 2017), Book Series: Advances in Intelligent Systems and Computing, 637 (2018), 199-208
[8] Galazka-Czarnecka, I.; Korzeniewska E., Czarnecki A. et al., Evaluation of Quality of Eggs from Hens Kept in Caged and Free-Range Systems Using Traditional Methods and Ultra-Weak Luminescence, Applied sciences-basel, 9 (2019), No. 12, 2430.
[9] Korzeniewska E., Walczak M., Rymaszewski J., Elements of Elastic Electronics Created on Textile Substrate, Proceedings of the 24th International Conference Mixed Design of Integrated Circuits and Systems, MIXDES 2017, 447-45.
[10] Szczęsny A., Korzeniewska E., Selection of the method for the earthing resistance measurement, Przegląd Elektrotechniczny, 94 (2018), No. 12, 178-181.
[11] Goclawski J., Korzeniewska E., Sekulska-Nalewajko J. et al., Extraction of the Polyurethane Layer in Textile Composites for Textronics Applications Using Optical Coherence Tomography, POLYMERS, 10 (2018), No. 5, 469
[12] Bartušek, K.; Drexler, P.; Fiala, P.; et al., Magnetoinductive Lens for Experimental Mid-field MR Tomograph, Progress in Electromagnetics Research, Symposium Location: Cambridge, MA JUL 05-08, (2010), 1047-1050
[13] Dušek, J.; Hladký, D.; Mikulka, J., Electrical Impedance Tomography Methods and Algorithms Processed with a GPU. In *PIERS Proceedings (Spring)*, (2017), 1710-1714, ISBN: 978-1-5090-6269-0
[14] Kak A.C., Slaney M., Principles of Computerized Tomographic Imaging, *IEEE Press, New York*, 1999
[15] Kłosowski G., Rymarczyk T., Using Neural Networks and Deep Learning Algorithms in Elecrical Impedance Tomography, *Informatyka, Automatyka Pomiary w Gospodarce i Ochronie Środowiska (IAPGOŚ)*, (2017), nr.3, 99-102
[16] Kłosowski G., Rymarczyk T., Gola A., "Increasing the Reliability of Flood Embankments with Neural Imaging Method", *Applied Sciences*, 8 (2018), (9), 1457
[17] Lawson Ch.L., Hanson R.J., Solving Least Squares Problems, *„Classics in Applied Mathematics"* (1995), 15, SIAM
[18] Mikulka, J., GPU- Accelerated Reconstruction of T2 Maps in Magnetic Resonance Imaging, *Measurement Science Review*, (2015), vol. 4, 210-218, ISSN: 1335-8871
[19] Smolik W., Kryszyn J., Olszewski T., Szabatin R., "Methods of small capacitance measurement in electrical capacitance tomography", Informatyka, Automatyka, Pomiary w Gospodarce i Ochronie Środowiska IAPGOS, vol. 7, (2017), no. 1, 105-110
[20] Koulountzios P., Rymarczyk T., Soleimani M., Ultrasonic Tomography for automated material inspection in liquid masses. 9th World Congress on Industrial Process Tomography, Bath, Great Britain, 2-6 Sept. (2018)
[21] Ming Yang, Schlaberg H.I., Hoyle B.S., Beck M.S., Lenn C., Real-Time Ultrasound Process Tomography for Two-Phase Flow Imaging Using a Reduced Number of Transducers, *IEEE Transactions on Ultrasonics, Ferroelectrics, and Frequency Control*, vol. 46, (1999), No. 3
[22] Rymarczyk T, Kłosowski G. Innovative methods of neural reconstruction for tomographic images in maintenance of tank industrial reactors. Eksploatacja i Niezawodnosc – Maintenance and Reliability, 21 (2019), No. 2: 261–267
[23] Polakowski, K., Filipowicz, S.F., Sikora, J., Rymarczyk, T., Quality of imaging in multipath tomography, *Przeglad Elektrotechniczny*, vol. 85, (2009), Issue 12, 134-136
[24] Rymarczyk T., Sikora J., Polakowski K., Adamkiewicz P., Efektywny algorytm obrazowania w tomografii ultradźwiękowej i radiowej dla zagadnień dwuwymiarowych, *PRZEGLĄD ELEKTROTECHNICZNY*, ISSN 0033-2097, R. 94 NR 6 (2018), doi:10.15199/48.2018.06.11 (in Polish)
[25] http://www.mathworks.com/products/matlab/ [access: June 2018]
[26] Dwinnell W., Data Mining in MATLAB, https://matlabdatamining.blogspot.com/2010/02/putting-pca-to-work.html [access: July 2019]